Approaches to Quantification of Microstructure for Model Lipid Systems

Baomin Liang[a], Jason L. Sebright[b], Yuping Shi[a], Richard W. Hartel[a,*], and John H. Perepezko[b]

Departments of [a]Food Science and [b]Materials Science and Engineering, University of Wisconsin–Madison, Madison, Wisconsin 53706

ABSTRACT: Semisolid fat samples with different solid fat contents and microstructures were prepared by crystallization of mixtures of model lipid systems containing high-melting and low-melting lipids and analyzed for microstructural properties. Microstructure images were acquired by confocal scanning light microscopy and showed fat crystals or fat crystal flocs combined with their surrounding continuous phase to constitute microstructural units and a microstructural network that was formed through their interaction. Fat crystal flocs and their centroids, microstructure units, and their interface boundaries were identified by image analysis. Several methods to quantify microstructure were compared. A new concept was introduced: the microstructure density, defined as the number of microstructural units per unit volume of the system. Also, the Richardson plot and particle counting methods (PCM) were used to find the fractal dimension of the crystal network. The Euler characteristic and nearest neighbor features of the microstructure were obtained as well by use of custom-developed programs. The different metrics of semisolid lipid microstructure were compared in terms of their physical meaning, means of acquisition, and consistency. The results showed that the quantitative microstructure parameters obtained from different approaches, except the fractal dimension determined by the PCM, can identify both differences and similarities of microstructural characteristics in the model lipid systems studied in this work.

Paper no. J11094 in *JAOCS 83*, 389–399 (May 2006).

KEY WORDS: Crystallization, crystal network, Euler characteristic, fractal dimension, image analysis, lipid, microstructure, microstructure density, Minkowski functionals, nearest neighbor analysis.

Semisolid lipid systems containing mixed high-melting and low-melting TAG are common in many food products. The properties (rheological, textural, functional) of these food products are related to both TAG composition and microstructure. From molecular and microscopic levels, processing conditions have significant effects on structure development and on the macroscopic properties (1–5). Solid fat content (SFC) is considered a primary factor that influences the rheological properties of a semisolid lipid system. High SFC generally leads to hard products as represented by a relatively high rheological modulus. However, two systems with the same SFC may have quite different rheological properties, indicating that the microstructure of the system also has an important impact on rheological properties (6,7). Therefore, it is generally accepted that rheological properties such as hardness and spreadibility may be quantitatively related to SFC and some microstructural factors.

A mechanical model of a simple fat network was originally developed by van den Tempel (8), in which the network is composed of straight chains of aggregated fat particles held together by van der Waals–London attraction that contributes the force to the modulus of the material. The particles that constitute the network are assumed to have simple shape and common orientation with uniform size. However, it was very difficult to describe the network properties quantitatively owing to the complex and random nature of the structure of a real system. Thus, quantification of microstructural characteristics of a semisolid lipid system becomes the key issue.

Vreeker (6) suggested that fat crystal networks had a fractal nature (9,10). The fractal dimension (10) was introduced to quantify the relationship between the mass of a cluster and its size. In studies on colloidal gels, Shih *et al*. (11) developed a scaling theory in which the gel network was considered to be a collection of fractal flocs packed throughout the sample. Later, Marangoni *et al*. (12,13) applied fractal concepts and scaling theory to model a viscoelastic lipid system. The fractal nature in fat crystal networks was discussed in a recent article (14). The number of particles was found to be a linear function of fractal size after logarithmic transformation, with a slope of fractal dimension D. Thus, D can be obtained from image analysis of microscopic images of crystal networks of a system with a so-called particle counting method (PCM) (13,14).

In addition to fractal scaling of the crystal network, the spatial distribution of the crystals in the crystal network can be quantified in other ways (15,16). Torquato (17) presented an overview of some of the methods that have been used in the analysis of materials.

A method for the analysis of spatial point distributions that has been developed relatively recently is based on ideas from integral geometry (18). The key to the analysis procedure is the use of geometric and topological quantities called Minkowski functionals. The analysis of point patterns and other spatial distributions with Minkowski functionals is efficient and robust and has been successfully applied to wide-ranging topics such as spinodal decomposition, fluid flow through porous media,

*To whom correspondence should be addressed at Dept. of Food Science, University of Wisconsin, 1605 Linden Dr., Madison, WI 53706.
E-mail: rwhartel@wisc.edu

and the large-scale structure of the universe (19). Minkowski functionals (also called intrinsic volumes or quermass integrals) are a group of integral geometric quantities that can be calculated from the integrals of the radii of curvature of a set of objects in space. In d-dimensional space, d+1 Minkowski functionals are needed to describe the objects in that space. In two dimensions, the three Minkowski functionals have direct and easily understood meaning: the total area of the objects, A; the total perimeter length of the objects, L; and the Euler characteristic, χ. The Euler characteristic is a well-known quantity in algebraic topology and in 2-D can be calculated as the number of connected objects minus the number of holes in those objects. It can be shown that the mean values of the Minkowski functionals form a complete set of geometric and topological measures of a set of objects and incorporate the same information found in 2-point and 3-point correlation functions.

Another method for the analysis of spatial point patterns is based on techniques to characterize interactions between objects existing in a space. The nearest neighbor rule based on Dirichlet tessellation and Delaunay triangulation provides an efficient geometric algorithm for the determination of distances between objects (15). The nearest neighbor distance is the parameter most commonly used to characterize spatial object patterns, but separation distance (defined as distance between edge points of two objects) may play an important role, particularly if the features are large compared with the distances between particles with varied shape, size, and orientation. In addition, the number of nearest neighbors is of interest in analysis of space-filling structures (20).

In this work, different approaches to the quantification of the microstructures of model lipid systems are presented. The concept of microstructure density is introduced to express the microstructural characteristics of lipid materials quantitatively. Fractal dimensions are calculated using both the Richardson plot and the PCM. The Euler characteristic is used to quantify the spatial distribution of the crystal fat flocs. Nearest neighbor analysis is used to acquire relevant parameters for the microstructure. These approaches for microstructure quantification of semisolid lipid are also compared in terms of their physical meaning, means of acquisition, and consistency.

EXPERIMENTAL PROCEDURES

Materials. Two types of fat with different molecular compositions and melting properties were prepared for this study. High-melting lipid B containing mixed tri- and disaturated TAG with a melting point of 56.4ºC was a palm oil stearin produced by fractionation in our laboratory. The major TAG in lipid B, constituting about 93% of the mass, were PPP, POP, and OOP, where O = Oleic and P = Palmitic. Low-melting lipid E containing long-chain unsaturated (18:2) TAG with a melting point of 29.3ºC was purified from sunflower oil. The major TAG in lipid E, constituting about 73% of the mass, were LLL and LOL, where L = Linoleic. The TAG composition of these lipids was analyzed with a Hewlett-Packard (Wilmington, DE) 5890 GC system based on the method of Lund (21) with slight modification of the temperature program. TAG groupings of the materials are shown in Table 1.

TABLE 1
TAG Composition (g/100 g identified TAG) of Lipids B and E Used in this Work in Terms of Groups

TAG group	Lipid B	Lipid E
Short-chain, $\leq C_{40}$	3.8	2.7
$C_{42} + C_{44}$	0.1	0.0
Trisaturated long-chain in C_{46}–C_{54}	37.7	0.1
Disaturated long-chain in C_{46}–C_{54}	37.8	2.6
Monosaturated long-chain in C_{46}–C_{54}	17.4	21.8
Triunsaturated long-chain in C_{46}–C_{54}	3.3	72.8

Sample preparation. Lipid mixtures were prepared by mixing high- and low-melting lipids at a mass ratio of 50:50 (B/E). Lipid mixtures were melted at 80ºC for 1 h, and Nile Red was added at a level of 0.005%. It has previously been shown that this level of Nile Red has no effect on lipid crystallization (22). The melt was cooled statically to the crystallization temperature of 36°C in a jacketed stainless steel beaker connected to a water bath. Agitation was applied for 30 s to induce nucleation, followed by growth of fat crystals under static conditions at the same temperature for about 2 h. To obtain semisolid fat samples with similar SFC but different microstructures for lipid mixtures (five systems labeled as I through V with 3 or 4 replicates for each), different agitation speeds (0—1000 rpm) that induced different number of nuclei were used. Higher agitation speeds led to smaller crystal sizes. After the primary crystallization (about 2 h), samples of the slurry from the crystallizer were placed on microscope slides and in NMR tubes, and stored in a temperature-controlled chamber at 0ºC for secondary crystallization.

Microstructure imaging. Confocal scanning light microscopy (CSLM) was used to acquire images of microstructure of each semisolid fat. Compared with the conventional microscope, CSLM has an important advantage in that the depth resolution is much better. Out-of-focus light is blocked by the confocal optics so that only a very thin focal plane is observed. The thickness of the optical sectioning is usually less than a couple of micrometers (23). Owing to the narrowness of the focal plane thickness, fat crystals are sectioned at different positions of spherulites so that only a sectional image of crystals can be shown and the true size of crystals is hard to obtain. On the other hand, overlap of crystals in images is limited, and collection of a series of optical sections at a well-defined distance less than 1 μm is made possible.

Lipid mixture samples with a thickness of 1.5–2.0 mm were placed on microscope slides and stored at 0°C to complete secondary crystallization. A Bio-Rad 1024 CSLM system (Bio-Rad Laboratories, Hemel Hempstead, United Kingdom) including a Nikon Eclipse microscope (Nikon Inc., Melville, NY) was used for microstructure imaging. Confocal scanning was carried out at a temperature of about 0°C. A 4× objective was used, and gray scale microstructural images of semisolid fat samples were obtained with the frame of acquired images having a dimension of 512×512 pixels or 3.367×3.367 mm.

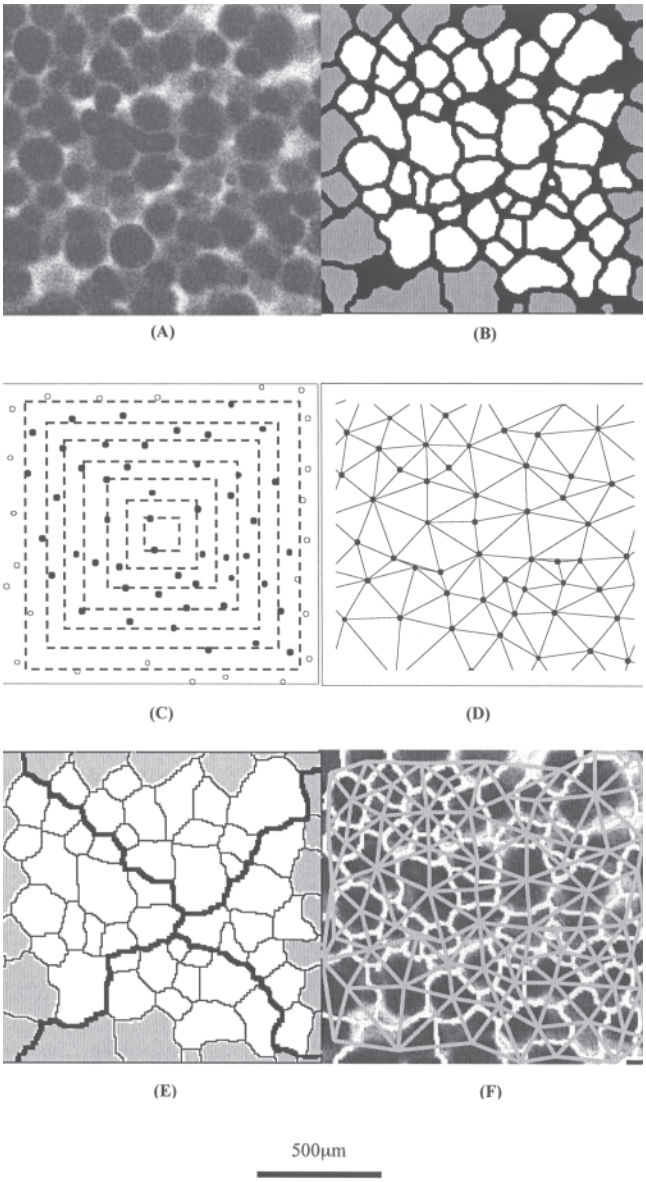

FIG. 1. Image examples to illustrate image analysis and microstructure quantification approaches. (A) Original confocal scanning light microscopy (CSLM) image of microstructure (part of a frame for clear illustration); (B) image of identified fat crystals and crystal flocs, those touching the frame shown in gray; (C) floc centroids shown as solid dots (●) for flocs not touching the frame and empty dots (○) for flocs touching the frame, dashed squares (---) showing regions with different scales for particle counting; (D) links and distances between nearest neighbor flocs; (E) image of microstructural units and their interface boundaries, those touching frame shown in gray, with representative interface boundaries closest to the diagonals shown in thickened lines; (F) combination of panels A through E showing the crystal network and the links of microstructural elements.

To test the effects of image resolution on the microstructure analyses in this study, a series of samples were repeated with images taken at two resolutions (512×512 and 1024×1024) for the same image dimension (3.367×3.367 mm). As discussed in the Appendix, differences in the results due to the increased resolution of the images were generally quite small (13.9% was the largest difference observed). Although ideally all samples would be analyzed with the highest resolution possible, the results shown in the Appendix indicate that a resolution of 512×512 is sufficient to document differences in methods of quantifying lipid crystalline microstructure in these model systems. Thus, the results presented here are for the lower magnification.

Measurement of SFC. SFC of duplicate samples after storage for 24 h at 0°C was determined with a Bruker minispec pc-120 nuclear magnetic resonance (NMR) system (Bruker, Milton, Ontario, Canada).

MICROSTRUCTURAL ANALYSES

An original image for a typical CSLM microstructure of the model lipid system is shown in Figure 1A. In this image, the liquid phase was labeled by Nile Red and appears as the bright areas, whereas solid fat or fat crystals, which were not labeled by Nile Red, appear as dark images. In this study, the nearly spherical fat crystals either existed individually or aggregated as crystal flocs. The individual spherical fat crystals had a relatively dense (dark) interior structure owing to the primary crystallization. The individual spherical fat crystals and/or crystal flocs were dispersed in a continuous phase (liquid oil). A 3-D illustration of the microstructure of this semisolid plastic fat is shown in Figure 2. Images of the microstructures of lipid systems by CSLM were the raw data for analysis. CSLM images were acquired on a certain section inside a semisolid lipid sample where fat crystals and crystal flocs were randomly arranged. The fat crystals/crystal flocs had complex shapes (not spherical or cubic), and the CSLM images were focused at different locations (center or off-center). Mean size and size distribution of crystals/crystal flocs could not be obtained by conventional stereological techniques (20). Instead, in this work, a "characteristic" crystal/crystal floc size was used. The characteristic size distribution of individual fat crystals or crystal flocs was found by image analysis from the CSLM images based on the area-based equivalent diameter for a circle in 2-D and a sphere in 3-D.

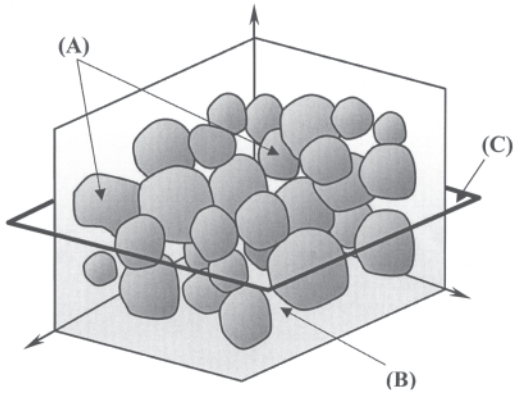

FIG. 2. Illustration of 3-D microstructure of semisolid plastic fat containing high-melting lipid (mixed tri- and disaturated TAG) and low-melting lipid [long-chain unsaturated (18:2) TAG]. (A) Fat crystals or crystal flocs; (B) liquid oil; (C) focus plane of CSLM.

Image analysis was performed using Optimas 6.1 (Optimas Corp., Bothell, WA) and ImageJ 1.32 (NIH, Bethesda, MD). The system was configured (area measurement method, etc.) and spatially calibrated (determination of mm per pixel), and the data collection parameters (parameters to be collected, data output file, etc.) were set. The original CSLM image (Fig. 1A) was treated to adjust contrast and brightness, if necessary, followed by image inversion based on the gray scale. Watershed separation (20) was performed with a fixed threshold (pixel gray level of 127 and 255) to distinguish solid fat and liquid oil according to the different gray scales and to distinguish fat crystals or crystal flocs in contact. Any hole in a floc area was filled, the edges of floc areas were smoothed, and point images that were not crystal flocs were removed. These procedures ensured that fat crystals and crystal flocs were correctly identified with correct areas. An image with identified fat crystals and crystal flocs was then generated (Fig. 1B). The identified flocs were digitized to obtain their areas and equivalent diameters, which were output to a Microsoft Excel spreadsheet for further treatment to determine the characteristic crystal size distribution (CCSD) based on the area of identified fat crystal flocs on the 2-D CSLM image. A major parameter of the CCSD was the characteristic mean area-based equivalent diameter d (mm). On average, about 2000 crystals or flocs (from 600 to 4000 depending on the number density of the crystals or flocs) were analyzed for each microstructure. Although the true size distribution could not be obtained, the general characteristics of the size distribution of crystals and flocs could still be represented in this way. The corresponding centroid data for the crystal flocs, which were the *x-y* locations for the center of their image pixels, were also obtained by image analysis. An example of the centroid is shown in Figure 1C.

Microstructure density. In this approach, each fat crystal or crystal floc combined with its surrounding continuous phase was defined as a microstructural unit. All microstructural units form networks through their interactions. The different microstructures of the model systems studied here were represented by how densely their microstructural units were arranged. Therefore, the concept of microstructure density is introduced to describe quantitatively the microstructural characteristics of these lipid systems. According to this definition, each microstructural unit in the semisolid fat systems had a characteristic size that was determined from a CSLM image after the individual fat crystals or crystal flocs were identified. A skeletonization technique (20) was used to divide the crystalline lipid microstructure into microstructural units based on the identified crystals or crystal flocs. The skeletonization function determined the mid-line in the space between any two identified features (e.g., the crystal flocs) to define interface boundaries of microstructure units. To ensure that microstructure units were correctly determined with correct sizes, broken borderlines were repaired and any branches on the borderline were pruned. Figure 1E is an image showing the determined microstructural units separated by lines. These lines represent boundaries of microstructure interfaces, which are in a 3-D space, on the 2-D CSLM focus plane. Areas representing the microstructural units were digitized and output to a Microsoft Excel spreadsheet for further treatment to obtain the microstructural unit size distribution (MUSD) including the area-based equivalent square length (or cube in 3-D), l_m (mm), and the number of microstructural units (N_m) in an image frame. Like CCSD, instead of a true size distribution, MUSD is also a representative or characteristic size distribution of these fat systems, as it is based on the particular aspect of the fat crystals or crystal flocs evident in the images.

To quantify the microstructure in a fat system, the microstructure density, d (mm^{-3}), was defined as the number of microstructural units per unit volume Since those fat crystals or crystal flocs and microstructural units touching the image frame were incomplete, they were not taken into account for analysis. To calculate microstructure density more reasonably, a reduced image frame length L_a (mm) was defined as

$$L_a = L - l_m \quad [1]$$

where L is the original dimension of the image frame (3.367 mm). In this way, microstructure density was obtained from

$$\delta = \frac{N_m{}^{1.5}}{L_a{}^3} \quad [2]$$

where $N_m{}^{1.5}$ (or $N_m{}^{3/2}$) approximates the number of microstructural units in a 3-D cubic space based on the corresponding 2-D square frames. It was noted that the numbers of microstructural units in a unit volume of two systems might be the same (i.e., they had the same microstructure density), even though their fat crystal/crystal floc sizes might be very different. To further distinguish the difference in microstructural characteristics between two such systems, a normalized microstructure density δ_n (mm^{-3}) was found by comparison to an ideal microstructure density δ_i (mm^{-3}).

An ideal microstructure density would be the number of microstructural units per unit volume of a system if all the crystals or crystal flocs in the system had the same size (i.e., the characteristic mean area-based equivalent diameter d), a spherical shape, and were packed in the densest way. For monosized spheres, the maximal packing density occurs in an ordered close-packed array with a coordination number of 12 (24). In this way, the microstructural unit will form a regular dodecahedron with a volume of $0.6938\ d^3$, and the ideal microstructure density will be

$$\delta_i = \frac{1}{0.6938 d^3} \quad [3]$$

In most cases with a relatively uniform size distribution of fat crystals or crystal flocs, δ_i was much larger than δ since the packing of fat crystals or crystal flocs in these systems was not ideal. To make microstructures of different systems quantitatively comparable, a normalized microstructure density, δ_n (mm^{-3}), was used to represent the overall microstructural characteristics of a system.

$$\delta_n = \frac{\delta}{\delta_i/\delta} = \frac{\delta^2}{\delta_i} \quad [4]$$

where the ratio δ_i to δ describes the extent of difference between the actual microstructure density of the systems and ideal microstructure density. A ratio that is closer to 1 implies that δ is closer to δ_i and, in general, means that the microstructural units are packed more densely. The normalized microstructure density reflects the effect of both the number and the size of fat crystals or crystal flocs on microstructure characteristics.

Euler characteristic. In an approach that is complementary to the microstructure density (which incorporates information on the number and sizes of the microstructural features), the Euler characteristic uses the number and positions of the microstructural features as the basis for characterization. Although the current discussion will be limited to two dimensions, this analysis technique can also be used for 3-D spatial distributions (25). The procedure for characterizing a 2-D point distribution using Minkowski functionals is straightforward. Given a list of (x,y) coordinates for a set of points, draw a square with sides of length l around each point (for this discussion squares will be used but the shape is arbitrary). Next, calculate the Minkowski functionals (i.e., total covered area, total perimeter, and Euler characteristic) for the set of squares. The Minkowski functionals as functions of length l give a quantitative description of the distribution of points. This procedure has several advantages over currently available methods for characterizing spatial point distributions. For example, no assumptions regarding the underlying point distribution are required. This procedure is also robust for small numbers (~500) of points (20). The latter point is quite significant because other methods (e.g., correlation functions) often require tens of thousands of points for analysis.

Another useful property of Minkowski functional analysis is that it can be easily performed on digital images (19,26). Owing to their additivity, the Minkowski functionals for the entire image can be calculated as the sum of the Minkowski functionals for each pixel in the image. After counting the number of covered pixels, n_s, the number of covered pixel edges, n_e, and the number of covered pixel vertices, n_v, the Minkowski functionals can be calculated as (26)

$$A = n_s \quad [5]$$

$$L = -4n_s + 2n_e \quad [6]$$

$$\chi = n_s - n_e + n_v \quad [7]$$

The mean values of the Minkowski functionals for a randomly distributed set of squares of edge length l are given by (26)

$$A = \Omega\,[l - \exp(-n)] \quad [8]$$

$$L = 4\,l\,N\exp(-n) \quad [9]$$

$$\chi = N\,(l - n)\exp(-n) \quad [10]$$

where A is the covered area, L is the perimeter length, χ is the Euler characteristic, Ω is the area of the calculation domain, N is the number of points in the calculation domain, ρ is the point density N/Ω, and $n = l^2\rho$. The shape drawn around each point is arbitrary, and it may be more convenient to use other shapes depending on the geometry of the sample or the computational grid; however, Equations 5–10 are only valid for squares, and different equations will be required for other shapes. The Euler characteristic is an especially sensitive measure of the spatial distribution (20) and this functional is used for the analyses in this paper. In Figure 3, a typical profile of Euler characteristic vs. length is shown that was the result of Euler characteristic analysis for the microstructure in a model system studied in this work (System I in Fig. 4). The sign of the Euler characteristic was chosen such that positive values correspond to black objects on a white background (i.e., when l is small) and negative values correspond to white objects on a black background (i.e., when l is large and the squares overlap creating isolated white regions). The four points on the χ vs. l curve that are used to characterize the lipid microstructures are the maximum and minimum Euler characteristic, the Euler minimum length, and the zero crossing length (Fig. 3).

Nearest neighbor analysis. To describe characteristics of correlation among crystals/crystal flocs, another parameter, nearest neighbor distance (NND) and its derivatives, was also used to quantify microstructure (15). This approach is based on a hypothesis that the microstructure and rheological-mechanical properties of a semisolid system are primarily related to interaction among the nearest neighbor microstructural units. Consequently, the distance between these nearest neighbor fat crystals or crystal flocs determines the extent of the interaction. According to the rule based on Dirichlet tessellation and associated Delaunay triangulation (15), the NND was defined as any distance between centers of two particles if it is shorter than any other distances that cross it. Thus, any crystal floc (particle) only links with its nearest neighbor flocs.

A custom computer program was developed to identify nearest neighbors for each fat crystal floc, to calculate the NND, and to generate statistical results of NND, including an average nearest neighbor distance (labeled as D_{NN}) and average number of neighbors (labeled as N_{NN}) for a system, based on the centroid data from the image analysis. An example of the nearest neighbor links based on NND results is shown in Figure 1D for the same microstructure illustrating the connectivity of fat crystals or crystal flocs. By taking into account the characteristic mean equivalent diameter of crystals or crystal flocs, an average separation distance (D_S) between nearest neighbor crystals or crystal flocs can be acquired from the following equation to describe the overall separation characters.

$$D_S = D_{NN} - d \quad [11]$$

Smaller values of D_{NN} and D_S and larger values of N_{NN} imply that fat crystals or crystal flocs are arranged close together and have more links and stronger interactions

Fractal dimension. Self-similarity is a characteristic of fractal objects that implies that geometric features of a fractal are the same at any magnification and exist at all length scales. Ir-

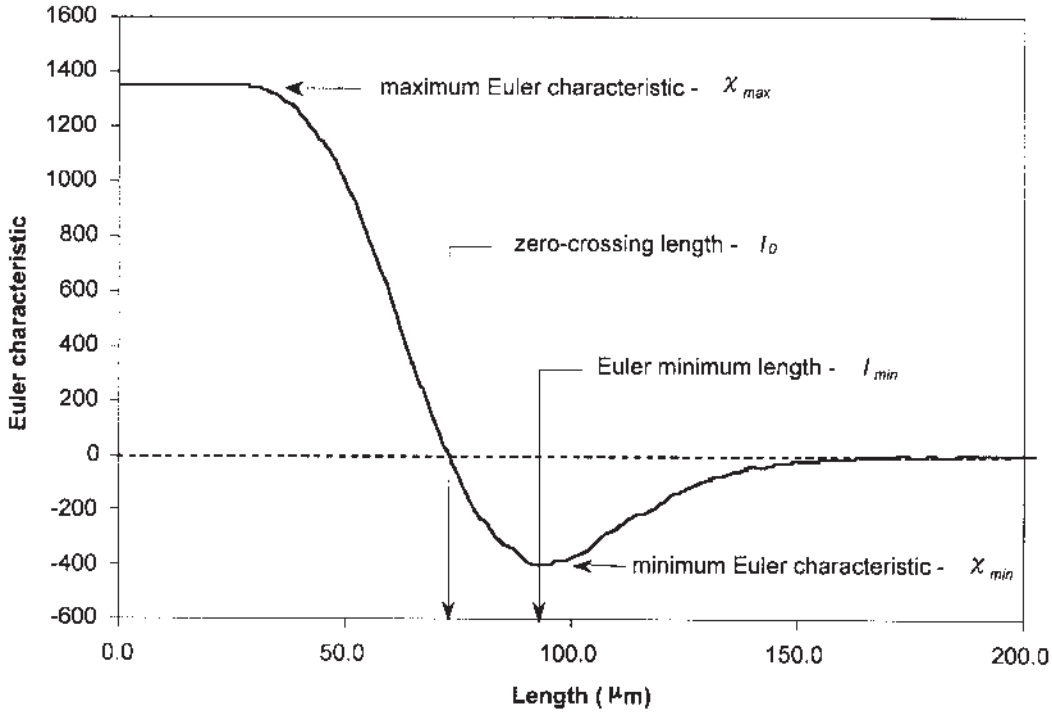

FIG. 3. Typical Euler characteristic curve as a function of length. The results shown are of Euler characteristic analysis for the microstructure in one of the replicates of System I shown in Figure 4.

regularity is another characteristic for certain fractal objects, and the extent of irregularity can be expressed as a fractal dimension of the objects. For the systems studied in this work, the interfaces between microstructure units existing in a 3-D space were considered to be fractal objects, and the method based on a Richardson plot (9,27) was used to calculate the fractal dimension of microstructure interfaces. Representative interface boundary lines that are closest to the diagonals were chosen for analysis, as shown in Figure 1E. The analytical format of the Richardson plot is

$$\ln L_f = c_L + (1-D_L)\ln \lambda \quad [12]$$

where λ is a measuring scale, L_f is the length of the fractal interface boundary measured with different λ , D_L is the fractal dimension of the interface boundary and c_L is a correlation coefficient for the lipid systems. Since there are fractal attributes for the spatially uniform systems and self-similarity exists in all dimensions, for the fractal interface in a 3-D space, the following equation is applicable:

$$\ln A_f = c_A + (2-D_A)\ln \lambda \quad [13]$$

where A_f is the area of the fractal interface measured with different λ, D_A is fractal dimension of the interface, and c_A is a correlation coefficient for the lipid systems. A specific relationship between D_A and D_L exists for a system uniform in all dimensions; however, further mathematical analysis is necessary to derive the relationship. A custom computer program was developed to calculate the length of boundary lines, establish the relationship between L_f and λ, and then determine D_L for the representative microstructure interface boundaries.

The PCM was also used to determine the fractal dimension based on polarized light microscopic images (13,14). In this work, centroid data of fat crystals or flocs were obtained from image analysis procedures as described earlier and then applied to PCM. If a fractal nature is assumed, there is a relationship between number of features and the corresponding measuring scale:

$$\ln N = c_N + D \ln R \quad [14]$$

where R is a length of scale for the analysis, N is the number of fat crystal flocs in the region corresponding to R, D is fractal dimension, and c_N is a correlation coefficient for our lipid systems. Figure 1C shows the PCM. The dots indicate locations of the crystal floc centroids, and the dashed squares show the counting regions with different scales from the center to the edge of image frame. Centroids falling within the analyzed region were taken into account. The scale length for crystal floc counting was performed with 32 pixels as both starting value and increment up to the whole frame (512 pixels). The fractal dimension D was then calculated according to Equation 14 to represent the microstructure characteristics.

RESULTS AND DISCUSSION

When the original image of microstructure (Fig. 1A) is combined with the images generated by analysis (Figs. 1B to 1E), a

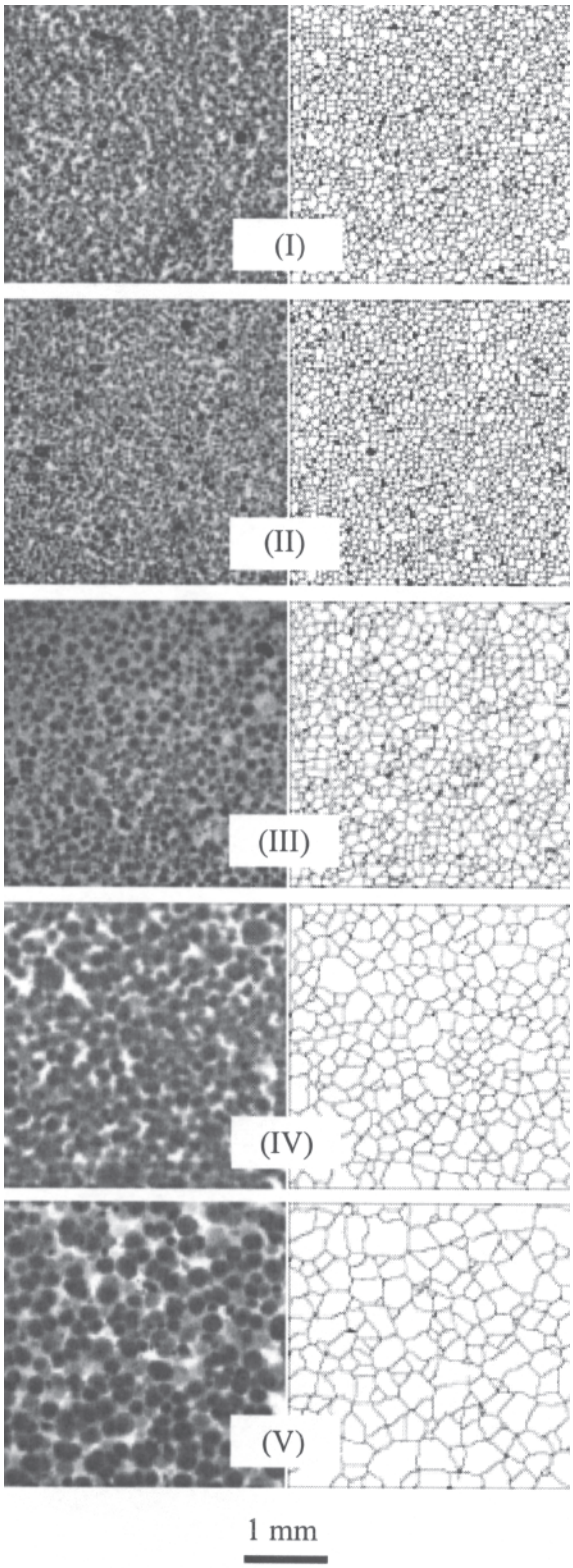

FIG. 4. Microstructures of five model lipid systems (B/E = 50:50) having different microstructural characteristics. The original CSLM image is on the left, and the image for obtained microstructure units with interface boundaries is on the right in each set. Lipid B: mixed tri- and disaturated TAG with a m.p. of 56.4°C made from palm stearin. Lipid E: long-chain unsaturated (18:2) TAG with a m.p. of 29.3°C from sunflower oil. For abbreviation see Figure 1.

whole view of the crystal network and the links of microstructural elements can be seen (Fig. 1F). A comparison of the different approaches for microstructure analysis was performed for a set of five lipid systems.

Figure 4 shows five sets of images (the original from CSLM on the left and the obtained microstructure units with interface boundaries on the right in each set) for five model lipid systems with different microstructure characteristics. Although the SFC of these systems was almost the same (about 0.36), they were crystallized at different conditions to generate the different microstructures. It can be visually seen that Systems I and II have the smallest particles and highest density, whereas System V has the largest particles and lowest density. The quantitative microstructure parameters corresponding to each system obtained from different analytical approaches and the *P*-values of ANOVA for each parameter among systems are given in Table 2.

The microstructure density and normalized microstructure density, as the terms suggest, reflect how densely the fat crystals/crystal flocs (the microstructural elements) are packed. From System I (or II) to V in Figure 4, microstructure density and normalized microstructure density change with a decreasing trend from about 1400 to 97 (mm^{-3}) and from about 250 to 34 (mm^{-3}), respectively. The microstructure density describes the density of features in a fat crystal/floc network in a clear and straightforward manner. In addition, the microstructure density directly incorporates information on the size and size distribution of the fat crystals and crystal flocs as a consequence of the method of calculation. This is in contrast to the Euler characteristic and fractal dimension analyses, which are based on relatively complex geometric ideas and do not directly include the size of the microstructural features.

Although the Euler characteristic itself is formally defined as an abstract idea in integral geometry (26), there are features of the Euler characteristic vs. length curves that can be directly related to characteristics in the microstructure. For example, the value of χ_{max} is simply the number of flocs in the image. χ_{min} and l_{min} are measures of the size of the voids between the flocs and are related to the nearest neighbor distance. The zero crossing length l_0 incorporates both the number of flocs (χ_{max}) and the distance between them (χ_{min}). This can be seen by considering l_0 as a point on a line with χ_{max} and χ_{min} as endpoints; changing either endpoint will change the zero crossing. From System I (or II) to V in Figure 4, χ_{max} and χ_{min} change with obvious decreasing/increasing trends from about 1300 to 206 and from about −340 to −34, respectively. This indicates that, from System I (or II) to V, the connectivity of particles in the network decreases. The zero-crossing length and Euler minimum length are parameters, with which enough number of particle connections makes the Euler characteristic reach a 0 and a minimum value, respectively. With more particles and higher density of their centroids in a system, distances between particles are shorter and they will connect to each other at smaller length, generate holes, and decrease χ in an Euler characteristic analysis. Therefore, zero-crossing length and Euler minimum length also describe the microstructure characteristics of a system

TABLE 2
Mean and SD of Quantitative Microstructure Parameters Obtained from Different Approaches and *P*-Value of ANOVA for Each Parameter for Model Lipid Systems with Different Microstructures[a]

System	I	II	III	IV	V	ANOVA	ANOVA
Label	5BE1	5BE2	5BE4	5BE5	5BE3	*P*-value	*P*-value
Replicates	3	3	3	3/4	4	(5 systems)	(I and II)
SFC [fractional]							
	0.367 ± 0.008	0.367 ± 0.007	0.357 ± 0.000	0.348 ± 0.008	0.346 ± 0.002	—	—
Microstructure density							
δ (mm^{-3})	1290 ± 43	1474 ± 25	362 ± 91	147 ± 20	97 ± 21	4.47×10^{-11}	0.013
δ_n (mm^{-3})	252 ± 65	244 ± 8	120 ± 17	53 ± 7	34 ± 11	2.00×10^{-6}	0.857
Euler characteristic							
χ_{max}	1256 ± 16	1353 ± 27	528 ± 130	281 ± 45	206 ± 40	1.48×10^{-10}	0.006
χ_{min}	−325 ± 16	−356 ± 27	−109 ± 5	−59 ± 13	−34 ± 7	2.27×10^{-11}	0.164
l_0 (mm)	82.1 ± 0.9	79.5 ± 0.7	123.3 ± 10.5	166.6 ± 7.5	195.8 ± 4.4	1.01×10^{-10}	0.016
l_{min} (mm)	107.2 ± 3.5	99.7 ± 2.7	115.4 ± 17.9	215.9 ± 12.2	245.0 ± 19.9	1.84×10^{-8}	0.043
Nearest neighbor feature							
D_{NN} (mm)	103.8 ± 0.9	99.8 ± 1.0	158.1 ± 16.1	216.1 ± 16.0	244.3 ± 23.9	2.76×10^{-7}	0.007
D_S (mm)	43.8	45.3	48.6	63.3	71.6	N/A	N/A
N_{NN}	6.00 ± 0.01	6.00 ± 0.01	5.92 ± 0.04	5.85 ± 0.03	5.81 ± 0.05	5.74×10^{-5}	0.965
Fractal dimension							
D_L	1.127 ± 0.004	1.125 ± 0.011	1.101 ± 0.007	1.094 ± 0.006	1.089 ± 0.007	1.45×10^{-10}	0.662
D	2.023 ± 0.089	1.997 ± 0.131	2.002 ± 0.083	1.932± 0.135	2.109 ± 0.288	0.769	0.785

[a]SFC, solid fat content; δ, microstructure density; δ_n, normalized microstructure density; χ_{max}, maximum Euler characteristic; χ_{min}, minimum Euler characteristic; l_0, zero-crossing length; l_{min}, Euler minimum length; D_{NN}, average nearest neighbor distance; D_S, average separation distance; N_{NN}, average number of nearest neighbors; D_L, fractal dimension of interface boundary of microstructure units; D, fractal dimension by particle counting method.

with lower l_0 and l_{min} representing higher connectivity. From System I (or II) to V in Figure 4, l_0 and l_{min} increase from about 80 to 196 μm and from about 104 to 245 mm, respectively, indicating decreased connectivity. As discussed previously, only the number and locations of particle centroids were taken into account for Euler characteristic analysis. For two systems with the same centroid characteristics (number and locations) but different particle sizes, the Euler characteristic parameters will be the same. In this work, all four Euler characteristic parameters (χ_{max}, χ_{min}, l_0, and l_{min}) changed over a reasonably wide range corresponding to the microstructures shown in Figure 4.

For nearest neighbor analysis, it is clear that a smaller nearest neighbor distance, or more precisely, the separation distance, illustrates how close to each other the particles are in a system. It is likely that there will be stronger interactions between close particles than with particles separated by larger distances. From System I (or II) to V in Figure 4, neighbor distance and separation distance change with an increasing trend from about 100 to 244 (mm) and from about 45 to 72 (μm), respectively. This implies that fat crystals/flocs in System I (or II) have stronger interactions than those in System V. The strength of the interactions can also be reflected by the number of nearest neighbors. If a particle has more nearest neighbors, it will have more connections and stronger interactions. Thus, the nearest neighbors of fat crystals/flocs from System I (or II) to V in Figure 4 change from 6.00 to 5.81. Although the absolute values for the difference in the number of nearest neighbors among systems are small, the differences are statistically significant in nearest neighbor analysis as verified by the ANOVA analysis. All the nearest neighbor analysis results (D_{NN}, D_S, and N_{NN}) have a very good trend that corresponds to the microstructures shown in Figure 4, indicating that this approach adequately quantifies lipid crystal microstructure in these systems.

For fractal dimension (D_L) based on the Richardson plot, a larger fractal dimension means the interface boundary line (of microstructure units) in a 2-D space has more zigzags or the interface in a 3-D space has more folds according to the concept of fractal geometry. In other words, the system has higher irregularity. It is understandable that there is a certain relation between this irregularity and the microstructure characteristics such as the density, shape, and size of particles. As the particle packing density increases for particles of irregular shape and small size, the interface of microstructure units built with these particles will have more folds and be more irregular. Thus, D_L values for the fat crystals/flocs network increase from 1.089 to 1.127 for Systems V to I (or II) shown in Figure 4. Like the number of nearest neighbors, there is a significant difference in the fractal dimension among systems, although the absolute value of difference is small. In this work, fractal dimension D_L was obtained from the 2-D interface boundary line. However, if 3-D images (e.g., combination of a series of microscopic images in the dimension perpendicular to the focal plane) with details are acquired, the digitized information and the fractal dimension of the interface can be found directly from analysis of these images. For fractal dimension by PCM, the ANOVA analysis shows there is no significant difference in this kind of fractal dimension among the systems. No trend was found to reflect the significant differences in the microstructure characteristics for systems shown in Figure 4. Thus, the fractal dimension determined by PCM was not able to distinguish the microstructure differences existing in the lipid systems studied in

TABLE 3
Correlation Coefficients of Quantitative Microstructure Parameters Obtained from Different Approaches[a]

	δ	δ_n	χ_{max}	χ_{min}	l_0	l_{min}	D_{NN}	D_S	N_{NN}	D_L	D
δ	1.000										
δ_n	0.979	1.000									
χ_{max}	0.997	0.992	1.000								
χ_{min}	–0.999	–0.985	–0.999	1.000							
l_0	–0.926	–0.974	–0.951	0.939	1.000						
l_{min}	–0.809	–0.892	–0.848	0.823	0.961	1.000					
D_{NN}	–0.938	–0.981	–0.961	0.948	0.999	0.958	1.000				
D_S	–0.824	–0.910	–0.864	0.843	0.976	0.990	0.970	1.000			
N_{NN}	0.944	0.985	0.966	–0.956	–0.998	–0.944	–0.998	–0.963	1.000		
D_L	0.984	0.994	0.992	–0.990	–0.955	–0.844	–0.961	–0.876	0.971	1.000	
D	–0.095	–0.131	–0.119	0.124	0.287	0.261	0.240	0.330	–0.264	–0.162	1.000

[a]For abbreviations see Table 2.

this work. Values for the fractal dimension calculated by PCM from this work are very consistent with those of Narine and Marangoni (13,14) with a value around 2.0. For evenly or uniformly arranged features in a 2-D space, the dimension based on Equation 14 should be Euclidian (i.e., 2). Thus, in terms of particle counting, the results indicate that the particle number and region scale do not have a clear fractal relationship.

It can be seen in Figure 4 that Systems I and II are microstructurally similar, but there are significant differences in microstructure characteristics among Systems I (or II), III, IV, and V. The *P*-values of ANOVA in a group of five systems for all quantitative microstructure parameters, except fractal dimension determined by the PCM, are much smaller than 0.05 (related to confidence level of 95%) whereas the *P*-values of ANOVA in a pair of Systems I and II are larger than or relatively close to 0.05 (much larger than those in a group of five systems). This indicates the quantitative microstructure parameters obtained from different approaches, except fractal dimension determined by the PCM, can appropriately identify both differences and similarities of microstructural characteristics in the model lipid systems studied in this work.

Correlation analysis for the quantitative microstructure parameters was performed and the obtained correlation coefficients for each pair of parameters are shown in Table 3. All parameters, except the fractal dimension by PCM, have very good correlation with one another with correlation coefficients of at least 0.8 (absolute) and mostly higher than 0.9 (absolute), indicating they are suitable to quantitatively describe the microstructure characteristics. Although not a focus of this work, it would be an interesting exercise to delve further into how each of these microstructural parameters are interrelated.

ACKNOWLEDGMENTS

Authors Liang, Shi, and Hartel gratefully acknowledge the United States Department of Agriculture for financial support via the National Research Initiative Competitive Grants Program, which made this work possible. Authors Sebright and Perepezko gratefully acknowledge the financial support of the National Aeronautics and Space Administration (NAG8-1278).

REFERENCES

1. deMan, J.M., and A.M. Beers, Fat Crystal Networks: Structure and Rheological Properties, *J. Texture Stud. 18*:303–318 (1987).
2. Juriaanse, A.C., and I. Heertje, Microstructure of Shortenings, Margarine and Butter—A Review, *Food Microstruct. 7*:181–188 (1988).
3. Heertje, I., Microstructural Studies in Fat Research, *Food Struct. 12*:77-94 (1993).
4. Marangoni, A.G., and R.W. Hartel, Visualization and Structural Analysis of Fat Crystal Networks, *Food Technol. 52*:46–51 (1998).
5. Aguilera, J.M., D.W. Stanley, and K.W. Baker, New Dimensions in Microstructure of Food Products, *Trends Food Sci. Technol. 11*:3–9 (2000).
6. Vreeker, R., L.L. Hoekstra, D.C. den Boer, and W.G.M. Agterof, The Fractal Nature of Fat Crystal Networks, *Colloids Surf. 65*:185–189 (1992).
7. Narine, S.S., and A.G. Marangoni, Factors Affecting the Texture of Plastic Fats, *INFORM 10*:565–570 (1999).
8. van den Tempel, M., Mechanical Properties of Plastic Disperse Systems at Very Small Deformations, *J. Colloid Sci. 16*:284–296 (1961).
9. Mandelbrot, B.B., *The Fractal Geometry of Nature*, W.H. Freeman, New York, 1977.
10. Meakin, P., Fractal Aggregates, *Adv. Colloid Interface Sci. 28*:249–331 (1988).
11. Shih, W.H., W.Y. Shih, S.I. Kim, J. Liu, and I.A. Aksay, Scaling Behavior of the Elastic Properties of Colloidal Gels, *Phys. Rev. A 42*:4772–4779 (1990).
12. Marangoni, A.G., and D. Rousseau, Is Plastic Fat Rheology Governed by Fractal Nature of the Fat Crystal Networks? *J. Am. Oil Chem. Soc. 73*:991–994 (1996).
13. Narine, S.S., and A.G. Marangoni, Fractal Nature of Fat Crystal Networks, *Phys. Rev. E 59*:1908–1920 (1999).
14. Marangoni, A.G., The Nature of Fractality in Fat Crystal Networks, *Trends Food Sci. Technol. 13*:37–47 (2002).
15. Diggle, P.J., *Statistical Analysis of Spatial Point Patterns*, Academic Press, London, 1983.
16. Ripley, B.D., *Spatial Statistics*, John Wiley & Sons, New York, 1981.
17. Torquato, S., Statistical Description of Microstructure, *Ann. Rev. Mat. Res. 32*:77–111 (2002).
18. Santalo, L.A., *Integral Geometry and Geometric Probability*, Addison-Wesley, Reading, MA, 1976.
19. Mecke, K.R., Integral Geometry in Statistical Physics, *Int. J. Mod. Phys. B 12*:9, 861–899 (1998).

20. Russ, J.C., *The Image Processing Handbook*, CRC Press, New York, 2002, pp. 383–526.
21. Lund, P., Analysis of Butterfat Triglycerides by Capillary Gas Chromatography, *Milchwissenschaft 43*:159–161 (1988).
22. Herrera, M.L., and R.W. Hartel, Effect of Processing Conditions on Physical Properties of a Milk Fat Model System: Microstructure, *J. Am. Oil Chem. Soc. 77*:1197–1204 (2000).
23. Blonk, J.C.G., and H. van Aalst, Confocal Scanning Light Microscopy in Food Research, *Food Res. Int. 26*:297–311 (1993).
24. German, R.M., *Particle Packing Characteristics*, Metal Powder Industries Federation, Princeton, NJ, 1989, pp. 4–5.
25. Mecke, K.R., T. Buchert, and H. Wagner, Robust Morphological Measures for Large-Scale Structure in the Universe, *Astron. Astrophys. 288*:697–704 (1994).
26. Michielsen, K., and H. DeRaedt, Integral-Geometry Morphological Image Analysis, *Phys. Rep. 347*:461–538 (2001).
27. Rahman, M.S., Physical Meaning and Interpretation of Fractal Dimensions of Fine Particles Measured by Different Methods, *J. Food Eng. 32*:447–456 (1997).

[Received March 22, 2005; accepted January 30, 2006]

APPENDIX

Effect of Image Resolution on Microstructure Quantification

Semisolid fat samples with five different microstructure densities (low, medium-low, medium, medium-high, and high) containing model lipids B and E were prepared following the procedures and covering the range of microstructure density for systems as described in the paper. These samples had similar microstructural characteristics (but not exactly the same) as samples I–V in the main body of this work. For this Appendix, however, the primary focus was to ascertain the effects of image resolution on the microstructural parameters.

The samples were examined by CSLM in the same way as described previously and images of the microstructure were obtained with both high (1024×1024) and low (512×512) resolutions for the same image frame (3.367×3.367 mm). Figure A1 shows the same frame imaged at the two resolution levels. The image analysis techniques introduced in the paper were performed on these images, and quantitative microstructure parameters were obtained. Figure A2 shows the identified fat crystal flocs for a portion of the images in Figure A1. Since images with high resolution have more detailed information than those with low resolution, the same crystal floc in a low-resolution image might be identified as more than one in a high-resolution image, thereby resulting in larger particle number and hence, smaller average size.

The differences in the major quantitative microstructure parameters at low and high resolution were analyzed, and the results are shown in Table A1. Compared with high-resolution images, analysis of low-resolution images resulted in smaller values for microstructure density and fractal dimension of interface boundary but larger values for zero-crossing length and nearest neighbor distance. The difference in the fractal dimen-

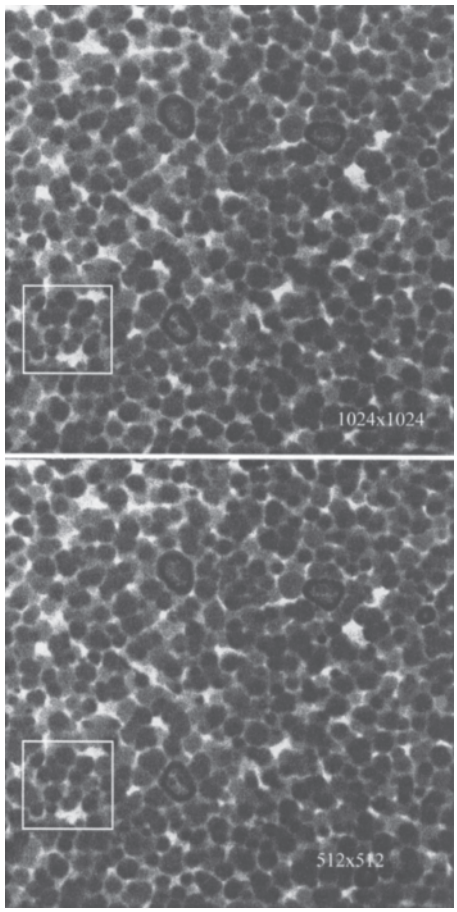

FIG. A1. Confocal scanning light microscopy images of semisolid fat with a medium microstructure density. Frame size: 3.367×3.367 mm.

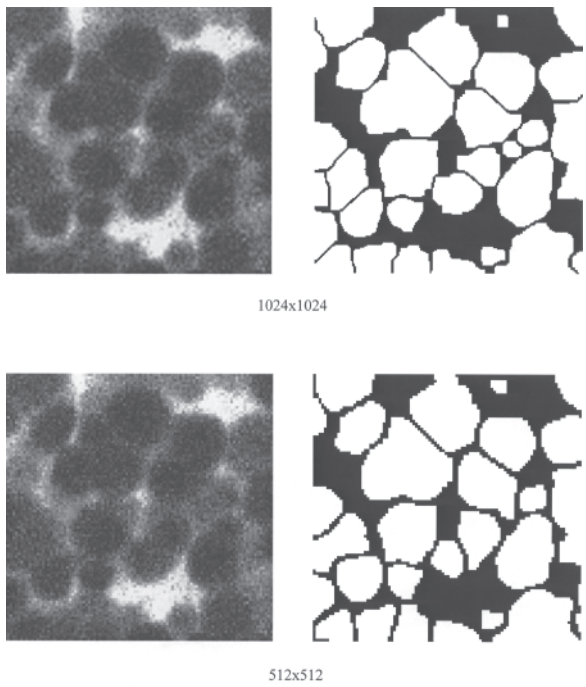

FIG. A2. Cropped box of Figure A1 with identified fat crystal flocs.

TABLE A1
Major Quantitative Microstructure Parameters and Average Percentage of Difference for Low (512 × 512) Resolution (Lo) vs. High (1024 × 1024) Resolution (Hi)

Parameter	δ_n (1/mm^3)		l_0 (μm)		D_L		D_{NN} (μm)		D	
Image resolution	Hi	Lo	Hi	Lo	Hi	Lo	Hi	Lo	Hi	Lo
Low[a]	14.5	12.9	306.4	316.5	1.096	1.084	367.1	374.5	1.732	1.717
Medium low[a]	33.7	27.9	203.4	207.3	1.111	1.101	244.3	251.8	2.036	1.897
Medium[a]	87.9	75.8	140.6	147.7	1.126	1.108	167.5	185.7	2.000	2.085
Medium high[a]	239.6	202.7	84.7	94.3	1.136	1.122	106.2	119.5	1.953	1.954
High[a]	372.1	327.8	66.4	75.5	1.149	1.125	83.6	94.5	1.985	1.946
Difference %	−13.9		7.1		−1.4		8.3		—	

[a]Microstructure density level for semisolid fat samples. For abbreviations see Table 2.

sion by PCM was negligible. The largest differences observed due to enhanced resolution were for the microstructural density term, δ_n, with a difference of 13.9%. The other parameters were different by less than 10%.

Correlation analysis was performed and the obtained correlation coefficients between high- and low-resolution images were 1.000, 1.000, 0.981, 0.999 and 0.803 for δ_n, l_0, D_L, $D_{NN,}$ and D, respectively. The high correlation coefficients and the definite (positive or negative) difference trend for each parameter (except the fractal dimension by PCM) documents that the 512 × 512 resolution was high enough to differentiate microstructures quantitatively and to give results that would be consistent with higher-resolution images for the studied model lipid systems.